

Significance of activation energy and quadratic radiative heat on magneto-Reiner-Rivlin nanofluid flow through a rotating disk

S Sandya¹, K Sreeram Reddy¹, P Sreehari¹

¹*Department of Mathematics, Osmania University, Hyderabad, Telangana 500007, India*

Corresponding author Email: pagidipallysrihari@gmail.com

Abstract: The study of enhancement of heat by non-Newtonian fluid has set up a capable and appropriate dome for technological application than the Newtonian fluid. A newly sort of Reiner-Rivlin fluid has been investigated through a revolving disk with Rosseland quadratic thermal radiation and magnetism. The mechanisms of activation energy and chemical reactions are also accounted. Two-component generalized Buongiorno nonliquid model comprising of haphazard motion and thermo-migration of nanoparticles is employed. The appropriate transmutation utilizes to simplify the flow model equations in the form of PDE's into ODE's. Terminology of wall skin friction and surface heat transfer have measured as well as deliberated for key parameters involved in the problem. The numerous consequences of scheming parameter on the Reiner-Rivlin nanofluid radial velocity, tangential velocity, temperature and concentration of nanoparticle profiles are portrayed graphically and deliberated in detail. Moreover, for the validation, the achieved results are renowned with previous literature in limiting case and obtained a good result. The outcome shows that the radial velocity gets decreased as the Reiner Rivlin fluid variable increases, while, an opposite effect is recorded for tangential velocity.

Keywords: MHD; Nanofluid; Reiner-Rivlin fluid; Viscous dissipation; Thermal radiation; Activation energy; Brownian motion.

Nomenclature

(r, ϕ, z)	Radial, circumferential, and longitudinal coordinates, respectively	T_r	Torque
(u, v, w)	Radial, circumferential, and longitudinal velocities respectively	$C_{f,r}$	radial skin friction coefficient
F', G	self-similar radial, and tangential velocities respectively	Ch	Chemical reaction parameter
C_p	specific heat capacity	q_r	radiative heat flux
k	thermal conductivity	E	Activation energy
b	a positive constant	Rd	Radiation parameter
s	stretching parameter		Greek Symbol
λ	Reiner-Rivlin fluid parameter	θ	Non-dimensional temperature
Pr	Prandtl number	μ	Dynamic viscosity
Nu_r	local Nusselt number	μ_c	Cross viscosity coefficient
Re	local Reynolds number	ν	kinematic viscosity
T	fluid temperature	η	Similarity variable
T_w	wall temperature	ρ	Fluid density
$C_{m,r}$	moment coefficient	ϕ	Azimuthally coordinate
Nb	Brownian motion	φ	Viscous dissipation
Nt	Thermophoresis force	Ω	Angular viscosity
T_∞	ambient fluid temperature		

1. Introduction

The Reiner-Rivlin nanofluid flow model offers a sophisticated approach to studying fluid dynamics over a rotating disk. It captures the unique interplay between nanofluids and the non-Newtonian properties of Reiner-Rivlin materials. Its significance in heat transfer analysis is profound, with applications ranging from advanced cooling systems in electronic devices to thermal regulation in high-speed machinery and efficient heat exchanger designs. This model is a vital tool for enhancing thermal performance in various engineering and industrial processes. The diverse applications of Reiner-Rivlin nano liquid flow have sparked significant interest, prompting extensive investigations by numerous researchers, encompassing various

aspects such as: **Ali et al.**[1] explored the role of bioconvection in enhancing thermal efficiency during the rotational flow of Reiner-Rivlin nanofluids over a disk with multiple slip conditions, incorporating non-Fourier heat conduction, binary chemical reactions, magnetic effects, and activation energy. Similarly, **Abdal et al.** [2] examined the impact of bioconvection and activation energy on Reiner-Rivlin nanofluid dynamics over a rotating disk with partial slip conditions, deriving coupled nonlinear differential equations based on the governing principles of Reiner-Rivlin fluids. **Alarabi et al.** [3] highlighted the superior thermal behavior of non-Newtonian fluids, specifically Reiner-Rivlin nanomaterials, for biomedical applications, focusing on gyrotactic microorganisms around an isothermal sphere with zero mass flux on the surface. **Puspanathan et al.** [4] investigated swirling flow patterns around a radially shrinking rotating disk using a Reiner-Rivlin fluid, solving the governing equations numerically with the `bvp4c` solver in MATLAB, and their findings aligned with established results on Von-Kármán flow for non-Newtonian fluids. **Rashid and Mustafa** [5] analyzed viscous heating effects in Reiner-Rivlin fluid flow over a stretchable rotating surface, incorporating a quadratic surface temperature distribution to model the disk's heating process effectively. **Khan et al.** [6] conducted a thermal bioconvective analysis of magnetized Reiner-Rivlin nanofluids, emphasizing the role of microorganism suspension in maintaining stability and consistent performance. Their findings highlight the influence of radiative effects and external heat sources on thermal behavior. **Sabu et al.** [7] numerically investigated the thermodynamic properties of Reiner-Rivlin nano liquids over a rotating disk, employing a non-homogeneous two-phase nanofluid model to examine the impact of nanoparticles and integrating temperature- and space-dependent heat sources. Using the von-Karman similarity technique and finite difference methods, they analyzed heat and mass transfer under boundary conditions involving velocity slip, volume fraction jump, and temperature jump. **Khan et al.** [8] extended this exploration to hydromagnetic bioconvective chemically reactive flows, incorporating

entropy generation analysis with contributions from Joule heating, radiation, dissipation, and the Soret effect, solved through the ND-solve technique. **Galal et al.** [9] focused on free convective flow near a rotating stretchable disc, incorporating Stefan blowing and Cattaneo–Christov fluxes, thermophoresis, random nanoparticle motion, and uniform magnetic fields. Their study applied Reiner-Rivlin liquid constitutive equations in cylindrical coordinates. Another study by **Khan et al.** [10] examined irreversibility in hydromagnetic flows over a rotating disk, analyzing entropy through thermodynamic laws and addressing Brownian motion, thermophoresis, and heat generation mechanisms like Joule heating and radiation. Lastly, **Yu-Pei et al.** [11] introduced a novel analysis of Reiner-Rivlin nanofluids over a rough, rotating disk in porous media, employing the Cattaneo–Christov heat flux model to underline their superior heat transfer capabilities compared to Newtonian fluids.

In the realm of thermal sciences, the interplay between binary chemical reactions and activation energy unveils a captivating dimension of control over nanofluid behaviors, bridging the gap between molecular kinetics and macroscopic heat transfer phenomena. These intricate processes are pivotal in tailoring the efficiency of advanced thermal systems, where precise modulation of chemical pathways enhances the performance of energy devices and biomedical applications. Numerous researchers have made significant contributions to the study of activation energy, encompassing diverse perspectives and methodologies, including pioneering works, **Khan et al.** [12] analyzed the influence of modified activation enthalpy and radiation effects on heat transfer phenomena while examining mass transfer through thermophoretic effects, chemical reactions, and activation energy, employing the von Kármán similarity solution solved via the shooting method. **Ramasekhar et al.** [13] emphasized the significance of heat transfer in engine oil embedded with copper nanoparticles over a porous rotating disk, integrating magnetohydrodynamics, nonlinear thermal radiation, thermophoresis, and Brownian motion, utilizing the Midrich technique in Maple software for aerospace

applications. **Shafique et al.** [14] explored heat and mass transfer in the rotating flow of Maxwell fluid induced by a unidirectional stretching surface, incorporating a binary chemical reaction and activation energy modelled through a modified Arrhenius function while employing traditional boundary layer approximations for simplification. **Ijaz Khan et al.** [15] numerically investigated binary chemical reactions coupled with activation energy in a rotating flow with nonlinear heat flux and the inclusion of heat sources and sinks. **Latif Ahmad et al.** [16] adopted a mathematical modelling approach to characterize the swirling flow of Cross fluid on a rotating cylindrical disk, integrating Lorentz forces and low Reynolds number effects while addressing heat and mass transfer influenced by heat sources, sinks, and activation energy. **Sahoo and Nandkeolyar** [17] presented a mathematical study on magnetohydrodynamic radiative Casson nanofluid flow generated by stretching and coaxially rotating disks within a non-Darcy porous medium, incorporating Hall current effects and heat generation, solved using the successive linearization method (SLM).

The interplay between quadratic thermal radiation and nanofluid flow over a spinning disk presents a fascinating realm of study with profound implications for cutting-edge applications. As nanofluids, known for their superior heat transfer characteristics, engage with the nonlinear effects of thermal radiation, they open doors to innovative solutions in fields such as aerospace engineering, electronics cooling, and sustainable energy systems. By unravelling the complex dynamics of this interaction, researchers aim to unlock new possibilities for optimizing heat management, where precision in energy dissipation and efficiency is increasingly vital. Recent research has significantly advanced our understanding of nanofluid flow over spinning disks, particularly concerning the effects of quadratic thermal radiation. **Madhu et al.** [18] examined the influence of quadratic thermal radiation and activation energy on the flow of hybrid nanofluid at the oblique stagnation point across a cylinder using the Runge-Kutta Fehlberg 45 numerical method. **Jiannet al.** [19] investigated the effect of melting on Carreau fluid flow over a stretchable cylinder, with particular attention to the role of quadratic thermal radiation, utilizing similarity variables and the Homotopy Analysis Method (HAM) to derive semi-

analytical solutions to the governing equations. **Lavanya et al.** [20] explored entropy generation minimization in Carreau nanofluid flow over a convectively heated inclined plate, incorporating quadratic thermal radiation and chemical reactions for Stefan-blowing applications. **Rana et al.** [21] studied the time-dependent heat transport and nonlinear thermal buoyancy-driven flow of MWCNT-MgO-EG hybrid nanofluid at the stagnation point of a rotating sphere, subjected to thermal jump boundary conditions, while also examining quadratic density-temperature variations and quadratic Rosseland thermal radiation, with experimental data for MWCNT-MgO-EG viscosity and thermal conductivity used in finite element analysis. The study also highlighted the significant impact of the nonlinear Boussinesq approximation on the flow and heat transport characteristics of the working fluid. **Al-Kouz et al.** [22] examined the flow of non-Newtonian viscoelastic material driven by a stretching elastic sheet, considering the nonlinear Boussinesq approximation and quadratic Rosseland thermal radiation. **Islam et al.** [23] presented comprehensive double-hybrid nanofluid thermal conductivity models, including the Powell-Eyring fluid model with Carboxy-Methyl-Cellulose (CMC) and Carbon Nanotubes such as SWCNT and MWCNT. **Mahanthesh et al.** [24] conducted a numerical study on the boundary layer two-phase flow of Al₂O₃-H₂O nano liquid over a vertical flat plate, considering quadratic thermal convection and radiation, using the Khanafer-Vafai-Lightstone monophasic nanofluid (KVL) and Saffman's dusty fluid models to govern the flow of dusty nano liquids. Finally, **Sarkar et al.** [25] reported on heat transfer and entropy optimization in water/MoS₂-SiO₂ Casson hybrid nanofluid flow over an exponentially contracting permeable Riga surface under the influence of quadratic thermal radiation.

2. Mathematical Formulation

Consider a steady, incompressible MHD flow of Reiner-Rivlin nano liquid due to rotating disk subjected to Newton boundary conditions. The flow is in uniform rotation of the disk along vertical axis with stationary angular velocity Ω . The magnetic field is applied normal to the fluid motion. Let (u, v, w) be the component about the direction of (r, ϕ, z) correspondingly.

The Reiner-Rivlin in the form of stress tensor is given as:

$$\tau_{ij} = -p\delta_{ij} + \mu e_{ij} + \mu_c e_{ik} e_{kj} e_{jj} \quad (1)$$

δ_{ij} , μ , μ_c and e_{ij} is represented by Kronecker delta, dynamic viscosity of coefficient, cross-viscosity coefficient and deformation rate tensor. The mathematical formulation incorporates Rosseland quadratic thermal radiation and magnetism in the energy and momentum equations. Activation energy and chemical reaction effects are included in the concentration equation. A two-component generalized Buongiorno nonliquid model, considering Brownian motion and thermophoresis, governs nanoparticle transport. The governing equations are (See Ali et al. [26]).

$$\frac{\partial u}{\partial r} + \frac{u}{r} + \frac{\partial w}{\partial z} = 0 \quad (2)$$

$$u \frac{\partial u}{\partial r} - \frac{v^2}{r} + w \frac{\partial u}{\partial z} = \frac{\mu}{\rho} \frac{\partial^2 u}{\partial z^2} + \frac{\mu_c}{\rho} \left(\frac{\partial^2 v}{\partial z^2} \left(\frac{\partial v}{\partial z} - \frac{v}{r} \right) + \frac{\partial v}{\partial z} \left(\frac{\partial^2 v}{\partial z \partial r} - \frac{1}{r} \frac{\partial v}{\partial z} \right) + 2 \frac{\partial u}{\partial z} \frac{\partial^2 w}{\partial z^2} + \frac{1}{r} \left(\left(\frac{\partial u}{\partial z} \right)^2 - \left(\frac{\partial v}{\partial z} \right)^2 \right) \right) - \frac{\sigma B_0^2}{\rho} u \quad (3)$$

$$u \frac{\partial v}{\partial r} + \frac{uv}{r} + w \frac{\partial v}{\partial z} = \frac{\mu}{\rho} \frac{\partial^2 v}{\partial z^2} + \frac{\mu_c}{\rho} \left(\frac{\partial^2 u}{\partial z^2} \left(\frac{\partial v}{\partial z} - \frac{v}{r} \right) + \frac{\partial u}{\partial z} \left(\frac{\partial^2 v}{\partial z \partial r} - \frac{1}{r} \frac{\partial v}{\partial z} \right) + 2 \frac{\partial w}{\partial z} \frac{\partial^2 v}{\partial z^2} + 2 \frac{\partial v}{\partial z} \frac{\partial^2 w}{\partial z^2} \right) - \frac{\sigma B_0^2}{\rho} v \quad (4)$$

$$u \frac{\partial T}{\partial r} + w \frac{\partial T}{\partial z} = \tau \left[D_B \frac{\partial C}{\partial z} \frac{\partial T}{\partial z} + \frac{D_T}{T_\infty} \left(\frac{\partial T}{\partial z} \right)^2 \right] + \frac{1}{\rho c_p} \left[\left(k - \frac{32\sigma^* T_\infty^3}{3k^*} \right) \frac{\partial^2 T}{\partial z^2} + \frac{32\sigma^* T_\infty^2}{3k^*} \frac{\partial^2 (T^2)}{\partial z^2} \right] \quad (5)$$

$$u \frac{\partial C}{\partial r} + w \frac{\partial C}{\partial z} = D_B \frac{\partial^2 C}{\partial z^2} + \frac{D_T}{T_\infty} \frac{\partial^2 T}{\partial z^2} - K_r \left(\frac{T}{T_\infty} \right)^n \exp \left(\frac{E_a}{\kappa T} \right) (C - C_\infty) \quad (6)$$

Boundary conditions for the above problem are

$$u = ar, \quad v = \Omega r, \quad w = 0, \quad T = T_w, \quad D_B \frac{\partial C}{\partial z} + \frac{D_T}{T_\infty} \frac{\partial T}{\partial z} = 0 \quad \text{at } z = 0$$

$$u = 0, \quad v = 0, \quad w = 0, \quad T = T_\infty, \quad C = C_\infty, \quad \text{at } z \rightarrow \infty. \quad (7)$$

Introducing the following similarity transformations

$$\eta = \sqrt{\frac{\Omega}{\nu}} z, \quad u = r\Omega F', \quad v = r\Omega G, \quad w = -2\sqrt{\Omega\nu} F, \quad \theta(\eta) = \frac{T-T_\infty}{T_w-T_\infty}, \quad \phi(\eta) = \frac{C-C_\infty}{C_\infty} \quad (8)$$

By using above transformations (8) equations (2) -(6) reduces to

$$F''' + \lambda(F''^2 - G'^2 - 2F'F''') - F'^2 + G'^2 + 2FF'' - MF = 0 \quad (9)$$

$$G'' - 2F'G' + 2FG' + 2\lambda(F''G' - F'G'') - MG = 0 \quad (10)$$

$$(1 - 2Rd)\theta'' + 3Rd \left(\frac{(1 + (T_r - 1)\theta)\theta''}{+(T_r - 1)\theta'^2} \right) + 2Pr F \theta' + Pr(Nb\theta'\phi' + Nt\theta'^2) = 0 \quad (11)$$

$$\phi'' + 2ScF\phi' + \frac{Nt}{Nb}\theta'' - Sc\chi(1 + (\theta_r - 1)\theta)^n \exp\left(\frac{-E}{1 + (\theta_r - 1)\theta}\right)\phi = 0 \quad (12)$$

The associate boundary conditions are

$$F(0) = 0, \quad F'(0) = s = \frac{a}{\Omega}, \quad G(0) = 1, \quad \theta(0) = 1, \quad Nb\phi'(0) + Nt\theta'(0) = 0 \quad (13)$$

$$F' \rightarrow 0, \quad G \rightarrow 0, \quad \theta \rightarrow 0, \quad \phi \rightarrow 0 \quad \text{as } \eta \rightarrow \infty$$

where λ is Reiner-Rivlin fluid parameter, M is the magnetic parameter, Nb is Brownian motion factor, Rd is the thermal radiation factor, Nt is a thermophoretic parameter, δ is the temperature difference parameter, E is the non-dimensional activation energy, χ is the chemical reaction number, Sc is the Schmidt parameter, s is the stretching ratio factor and Pr is the Prandtl number.

$$\lambda = \left(\frac{\mu_c \Omega}{\mu} \right), \theta_r = \frac{T_w}{T_\infty}, M = \left(\frac{\sigma B_0^2}{\rho a} \right), R_d = \left(\frac{4\sigma^* T_\infty^3}{3k^* k} \right), Nb = \frac{\tau D_B (C_w - C_\infty)}{\nu}, Nt = \frac{\tau D_T (T_w - T_\infty)}{T_\infty \nu},$$

$$Sc = \frac{\mu}{\rho D_B}, Pr = \frac{\mu c_p}{k}.$$

Quantity of Engineering Importance

$C_{m,r}$, represent moment coefficient to measure the least amount of torque needed as; [37]

$$C_{m,r} = \frac{T_r}{\rho \Omega^2 r^5} \quad (14)$$

where T_r denotes the torque to keep the disk in uniform motion, which is explained as

$$T_r = \int_0^r \tau_{z\theta} \Big|_{z=0} 2\pi r^2 dr = \frac{\pi}{2} \rho \Omega \sqrt{\nu \Omega} (1 - 2\lambda F'(0)) r^4 G'(0). \quad (15)$$

The radial wall skin friction is given as:

$$C_{f,r} = \frac{\tau_{zr} \Big|_{z=0}}{\rho (\Omega r)^2} \quad (16)$$

The equation (15) and (16) becomes

$$Re_r^{1/2} C_{m,r} = \frac{\pi}{2} (1 - 2\lambda F'(0)) G'(0), \quad Re_r^{1/2} C_{f,r} = (1 - 2\lambda F'(0)) F''(0) \quad (17)$$

Local Nusselt number without radiative heat is given by:

$$Nu_r = - \frac{r \left[k \left(\frac{\partial T}{\partial z} \right) \Big|_{z=0} \right]}{k (T_w - T_\infty)}, \quad (18)$$

The equation (18) reduces to

$$Re_r^{-1/2} Nu_r = -\theta'(0), \quad (19)$$

3. Solution Methodology

The systems of Eqns. (9)-(12) with boundary conditions (13) are treated numerically by BVP4c. The simulation is found to furnish the solution of the above nonlinear problem. At the

first step, transmute the given system of nonlinear ODEs into first order ODE's. For the entire mechanism set new variables as follows

$$F = \Lambda_1, F' = \Lambda_2, F'' = \Lambda_3, G = \Lambda_4, G' = \Lambda_5, \\ \theta = \Lambda_6, \theta' = \Lambda_7, \phi = \Lambda_8, \phi' = \Lambda_9,$$

$$\Lambda_3' = \frac{(\lambda\Lambda_5^2 - \lambda\Lambda_3^2 + \Lambda_2^2 - \Lambda_4^2 - 2\Lambda_1\Lambda_3 + M\Lambda_1)}{(1 - 2\lambda P_2)} \quad (21)$$

$$\Lambda_5' = \frac{(2\Lambda_2\Lambda_4 - 2\lambda\Lambda_3\Lambda_5 - 2\Lambda_1\Lambda_5 + M\Lambda_4)}{(1 - 2\lambda\Lambda_2)} \quad (22)$$

$$\Lambda_7' = \frac{(-2Pr\Lambda_1\Lambda_7 - 3Rd(T_r - 1)\Lambda_7^2 - Pr(Nb\Lambda_7\Lambda_9 + Nt\Lambda_6^2))}{(1 - 2Rd + 3Rd(1 + (T_r - 1)\Lambda_6))} \quad (23)$$

$$\Lambda_9' = \left(ScCh(1 + \delta\Lambda_6)^n \exp\left[\frac{-E}{1 + \delta\Lambda}\right] \Lambda_8 - 2Sc\Lambda_1\Lambda_8 - \frac{Nt}{Nb}\Lambda_7' \right) \quad (24)$$

Subsequently, boundary conditions are

$$\Lambda_1(0) = 0, \Lambda_2(0) = s, \Lambda_4(0) = 1, \Lambda_7(0) = -Bi(1 - \Lambda_6(0)), Nb\Lambda_9(0) + Nt\Lambda_7(0) = 0 \\ \Lambda_2(\infty) = 0, \Lambda_4(\infty) = 0, \Lambda_6(\infty) = 0, \Lambda_8(\infty) = 0. \quad (25)$$

The boundary condition in Eq. (25) are calculated by the using of finite value for η_∞ as gives

$$F'(\eta_\infty) = 0, G(\eta_\infty) = 0, \theta(\eta_\infty) = 0, \phi(\eta_\infty) = 0 \quad (26)$$

The step size is taken $\Delta\eta=0.0001$ and convergent criterion are preferred to obtain numerical solution.

4. Result and Discussion.

To examine the impact of key parameters of the problem, Figs. 1-17 are plotted on $F'(\eta)$, $G(\eta)$, $\theta(\eta)$ and $\phi(\eta)$ for numerous values of suction parameter (s), Reiner-Rivlin fluid parameter (λ), magnetic field factor (M), thermophoretic parameter (Nt), Eckert number (Ec), Brownian motion factor (Nb), thermal radiation factor (Rd), Prandtl number (Pr), Schmidt number (Sc), chemical reaction factor (Ch), and activation energy factor (E). For the validation of the method employed in the current study is made by direct comparison see Table-1. A

contrast of $Re^{1/2}C_{f_r}$, $Re^{1/2}C_{m_r}$ and $F(\infty)$ is established with previous literature [37] in limited case which are in excellent agreement. Figs. 1-4 show the result of s parameter on radial velocity $F'(\eta)$, tangential velocity $G(\eta)$, temperature $\theta(\eta)$ and concentration $\phi(\eta)$ profiles. Fig. 1 shows that the effect of s on $F'(\eta)$ is augmenting function of s . Also, the radial component boundary layer structure increase with s . From the Figs. 2-4, it is noticed that the $G(\eta)$, $\theta(\eta)$ and $\phi(\eta)$ profiles show reducing behavior for enhancing value of s . Figs. 5-6 show the significance of Reiner-Rivlin fluid parameter on $F'(\eta)$ and $G(\eta)$. It is clear from Fig. 5, $F'(\eta)$ increases toward the disk with uplifted value of λ , while this trend is opposite for $G(\eta)$. Physically, near the disk an increment of viscoelasticity affects consequences in approaching more fluid in radial direction. Figs. 7-10 reveal the role of M on $F'(\eta)$, $G(\eta)$, $\theta(\eta)$ and $\phi(\eta)$ profiles. It can be shown from the figure that all profiles portray an asymptotic behavior. Figs. 7-8 revealed that larger value of M results in the reduction of both the radial $F'(\eta)$ and tangential $G(\eta)$ profiles. The stronger Lorentz force which develops drag force has the propensity to slow down the flow along the disk surface. This is shown that in Figs. 9-10 reduction in temperature $\theta(\eta)$ and concentration $\phi(\eta)$ profiles when the numeric values of M increased.

The importance of thermophoretic force (Nt) on temperature $\theta(\eta)$ and concentration of nanoparticles $\phi(\eta)$ field sketches is portrayed in Figs.11-12. It is observed from the Fig. 11 that the temperature field $\theta(\eta)$ and its boundary layer thickness uplifted for larger values of Nt . However, the concentration $\phi(\eta)$ displays depreciate with improving value of Nt (see Fig. 12). It is the fact that nanoparticles near the hot surface of the disk develop thermophoretic force, this force amplifies the temperature of the fluid in the liquid system. The behavior Ec and Rd on temperature profile $\theta(\eta)$ are plotted in Figs. 13-14. From Fig. 13, value of Eckert number Ec and Radiation parameter Rd is enhanced due to which the temperature profile is

also increased. It is also found that the thermal layer structure enhances with Ec and Rd . This is because, the radiative heat and viscous heat is encouraging for thermal boundary layer increment.

Figs. 15-18 displays the role of chemical reaction Ch , activation energy E , Schmidt number Sc and Brownian movement Nb on concentration of nanoparticles $\phi(\eta)$. Fig. 15 shows the features of chemical reaction parameter Ch on $\phi(\eta)$. It is found that the concentration of nanoparticles and its related boundary layer structure are reduced by larger Ch . From Fig. 16, the profile of concentration $\phi(\eta)$ grows for larger values of activation energy E . Infact E lessen the amend Arrhenius function which result promotes a generative chemical reaction this is because concentration is mounted. Figs. 17-18 represents the concentration of nanoparticles is a reducing function of Schmidt number Sc and Brownian motion factor Nb .

Table 2 presents the numerical data of $Re^{1/2}C_{fr}$ and $Re^{1/2}C_{mr}$ for various values of M , λ and s . It is found that the $Re^{1/2}C_{fr}$ and $Re^{1/2}C_{mr}$ decreasing property of M and they are increasing property of λ . Further, $Re^{1/2}C_{fr}$ is a decreasing property of s , owing to radial momentum layer thickness increased for larger values of s . Besides, the $Re^{1/2}C_{mr}$ is an increasing property of s . The numerical data of $Re^{-1/2}Nu_r$ for distinct values of M , λ , Nt , Nb , Rd , Ec , Ch , E and s are recorded in table 3. It is observed that the rate of thermal transport at the surface of the disc $Re^{-1/2}Nu_r$ is an increasing property of λ , Rd , E and s , while the rate of thermal transport at the surface of the disc $Re^{-1/2}Nu_r$ is a decreasing property of M , Nt , Ec and Ch .

5. Conclusion

The aim of current article is to examine the flow of Reiner-Rivlin nanofluid with Arrhenius activation energy due to rotating disk. The Key observations are under as follows.

- ❖ A reduction in radial outward flow is observed due to the Reiner-Rivlin parameter
- ❖ The impact of magnetism reduces the momentum layer structure.
- ❖ The thermal and solute layer structures diminished for stronger magnetism.
- ❖ The thermal layer structure improved via viscous heating mechanism.
- ❖ The haphazard motion of nanoparticles enhances the thermal boundary layer structure.

- ❖ Heat transfer increases with thermophoretic force Nt , thermal radiation Rd and Eckert number Ec .
- ❖ Heat transfer rate decrease as chemical reaction parameter Ch , while consequences of activation energy E extend it.

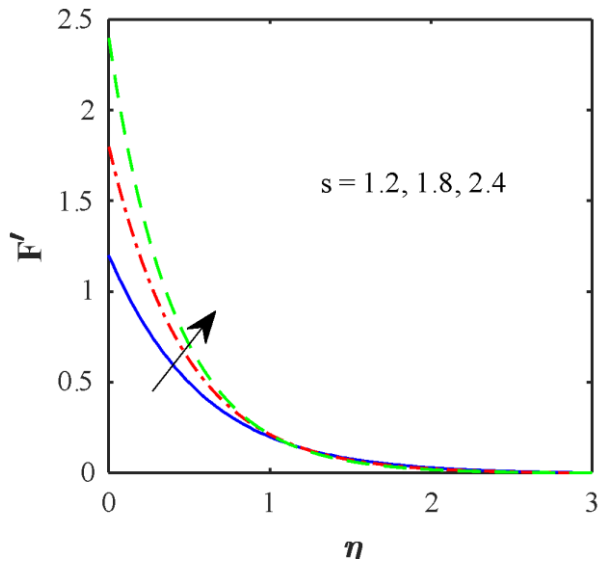


Figure-1. variations of F' via s

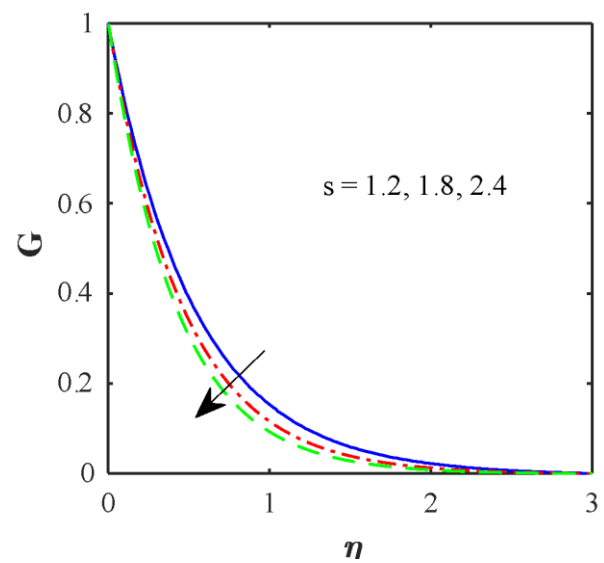


Figure-2. Variations of G via s

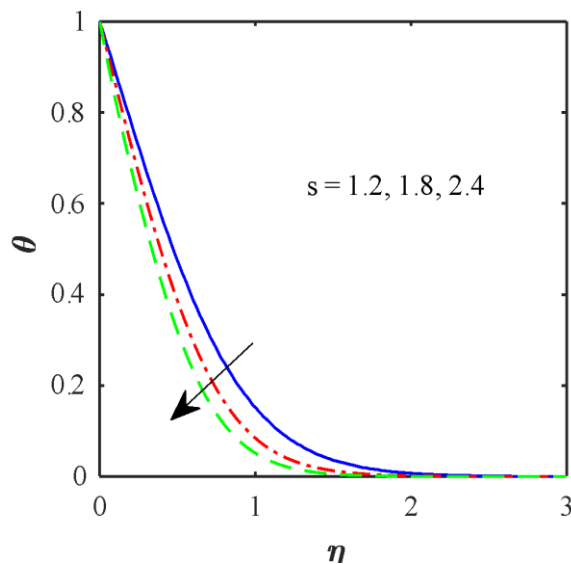


Figure-3. variations of θ via s

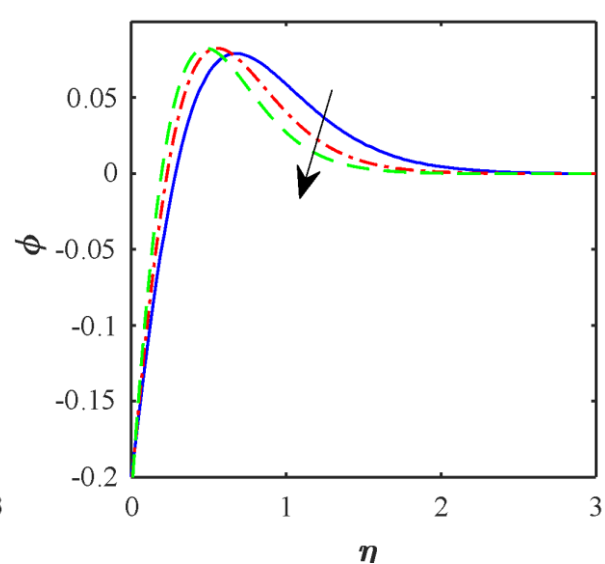


Figure-4. Variations of ϕ via s

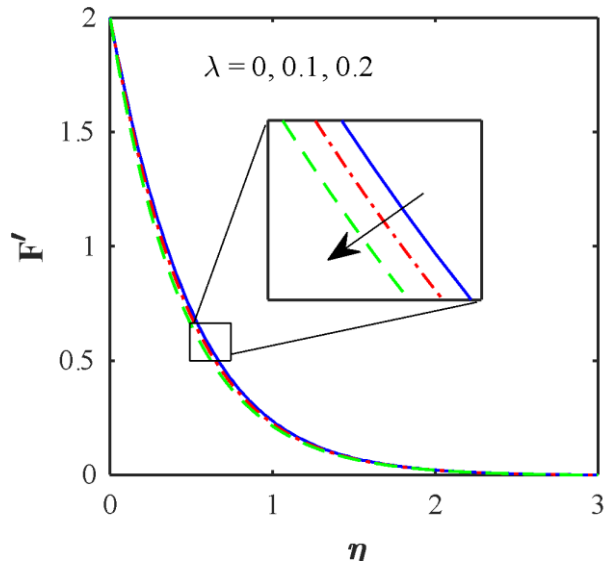


Figure-5. variations of F' via λ

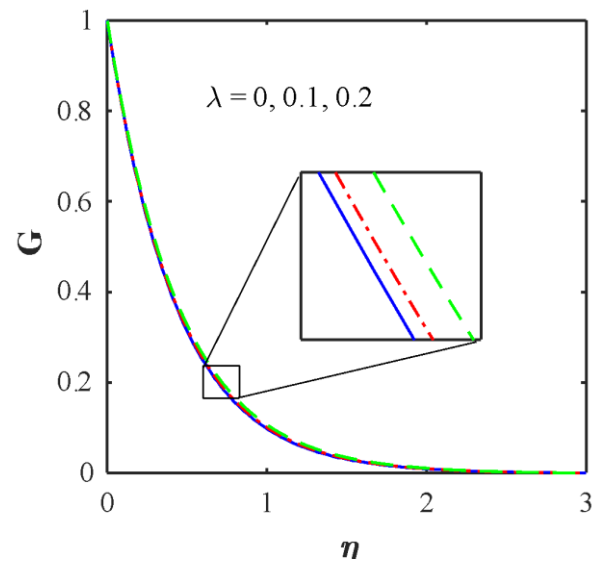


Figure-6. variations of G via λ

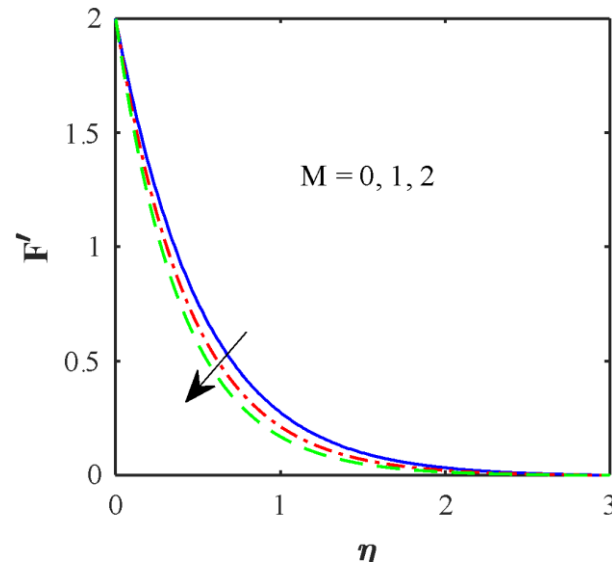


Figure-7. variations of F' via M

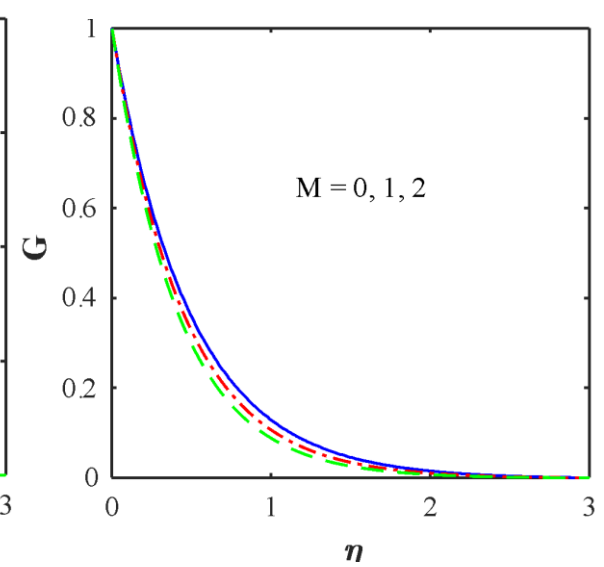


Figure-8. variations of G via M

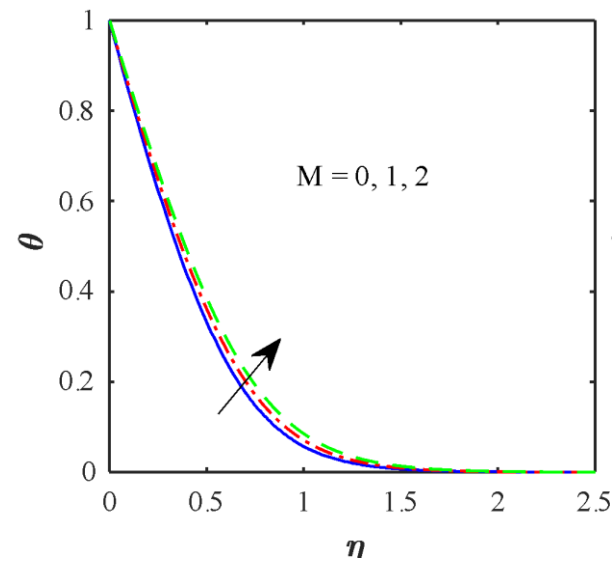


Figure-9. variations of θ via M .

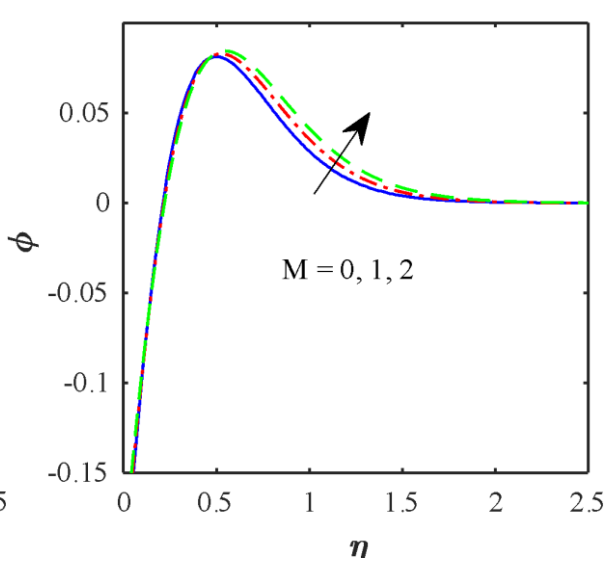


Figure-10. Variations of ϕ via M .

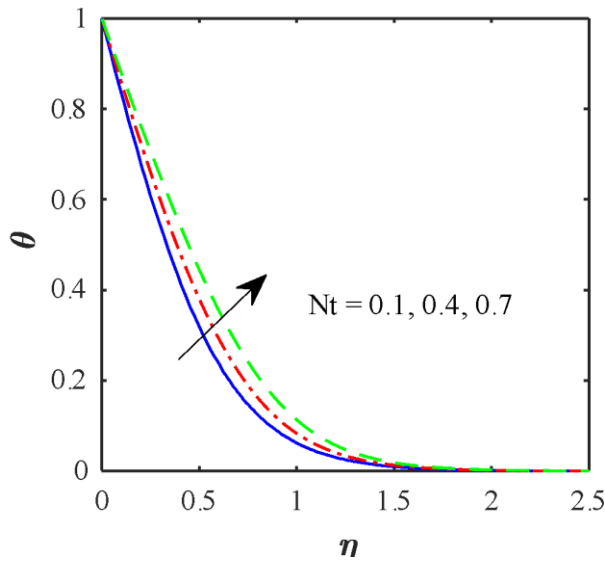


Figure-11. variations of θ via Nt

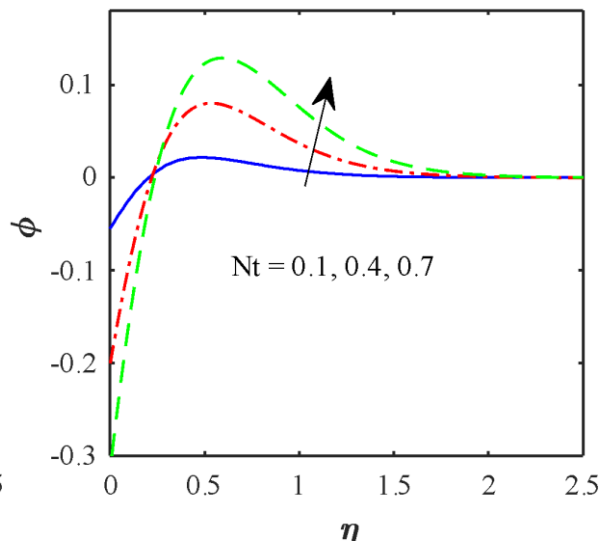


Figure-12. Variations of ϕ via Nt

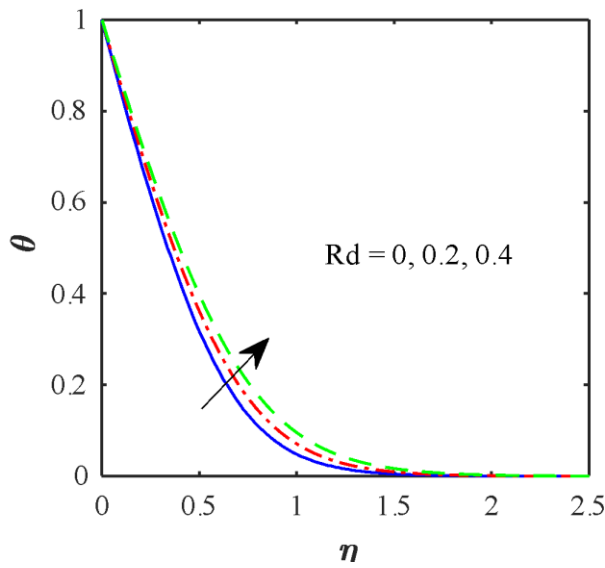


Figure-13. variations of θ via Rd

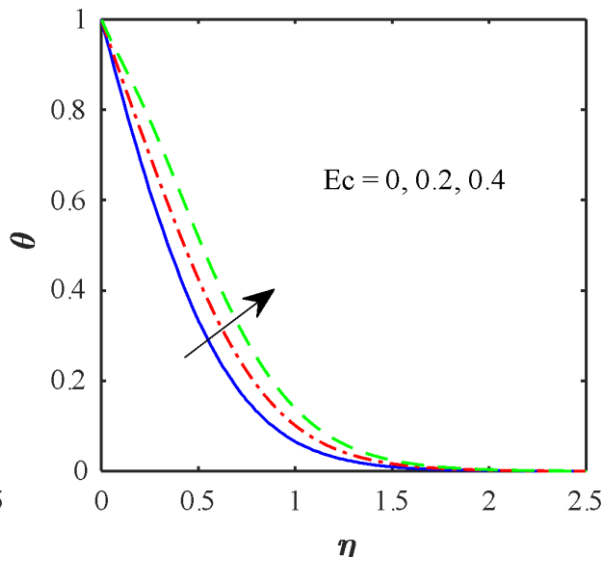


Figure-14. variations of θ via Ec .

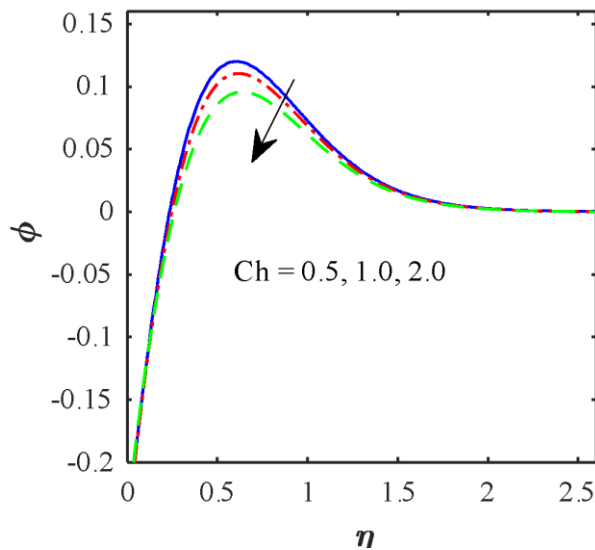


Figure-15. variations of ϕ via Ch

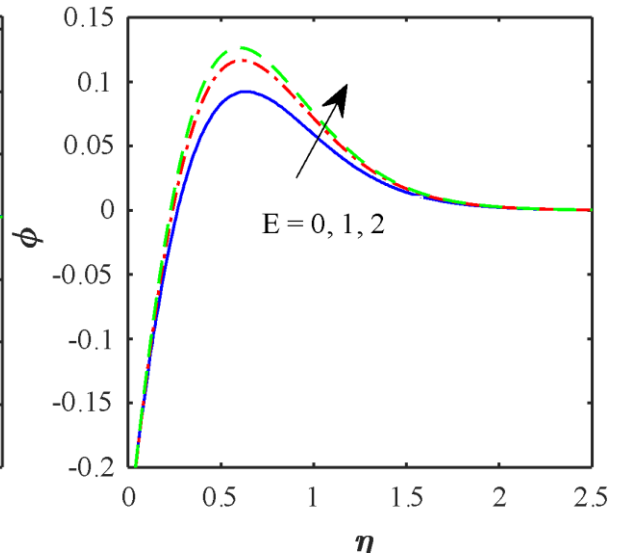


Figure-16. variations of ϕ via E

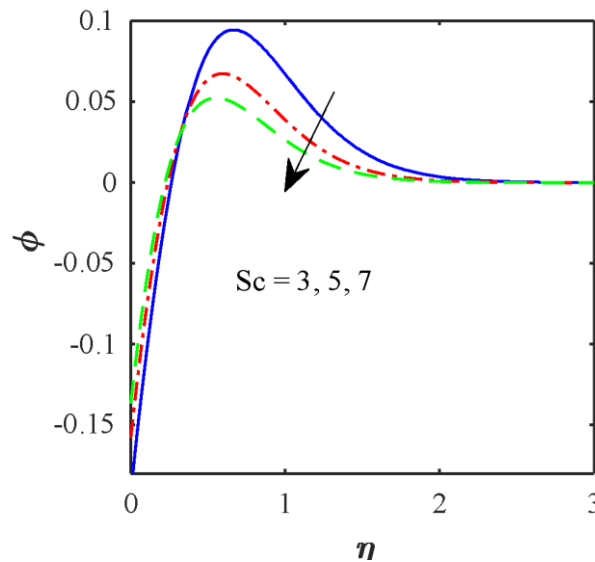


Figure-17. variations of ϕ via Sc

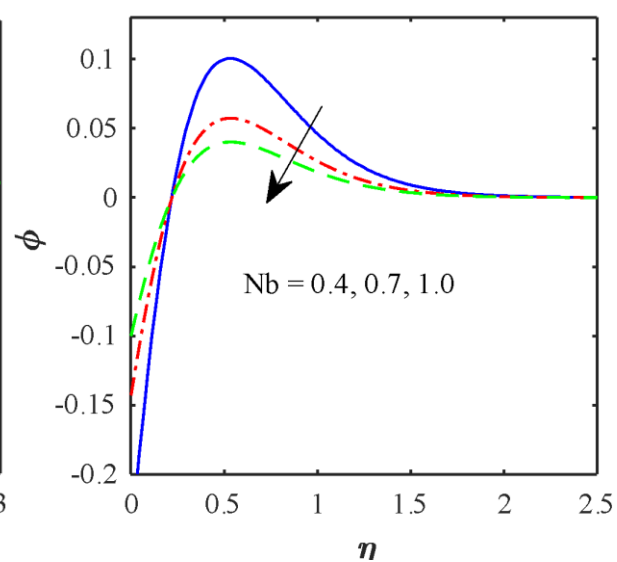


Figure-18. variations of ϕ via Nb

Table-1. Comparison of results by Rashid [37] and the present results when $M = 0, \lambda = 0.2$.

s	Previous Results [37]			Present Results		
	$Re^{1/2}C_{fr}$	$Re^{1/2}C_{m_r}$	$F(\infty)$	$Re^{1/2}C_{fr}$	$Re^{1/2}C_{m_r}$	$F(\infty)$
0.6	-0.251620	-1.446337	0.626431	-0.25149054	-1.44560827	0.62692223
1.0	-0.644825	-1.422921	0.758689	-0.64452142	-1.42265951	0.75774979
1.2	-0.784780	-1.340830	0.818382	-0.78473963	-1.34065425	0.81860672
1.4	-0.874302	-1.218939	0.873914	-0.87449797	-1.21881614	0.86825304

Table-2. Computational values of radial wall skin friction and moment coefficient.

M	λ	s	$Re^{1/2}C_{fr}$	$Re^{1/2}C_{mr}$
0.5	0.3	0.5	-0.2886	-1.4275
1.0			-0.4047	-1.6000
1.5			-0.5025	-1.7615
1.0	0.1		-0.4186	-2.0647
	0.3		-0.4047	-1.6000
	0.5		-0.3536	-1.1107
	0.3	0.6	-0.4939	-1.5283
		0.8	-0.6229	-1.3405
		1	-0.6720	-1.0986

Table-3. Computed values of the heat transfer rate for different values of flow parameters.

M	λ	Nt	Nb	Rd	Tr	Ch	E	s	$Re^{-1/2}Nu_r$
0.5	0.3	0.3	0.3	0.2	1.25	1	1	1	0.7700
1.0									0.7334
1.5									0.7018
1.5	0.10								0.7280
	0.25								0.7090
	0.40								0.6861
	0.3	0.2							0.7139
		0.4							0.6898
		0.6							0.6662
		0.3	0.2						0.7018
			0.4						0.7018
			0.6						0.7018
			0.4	0					0.9259
				0.1					0.7959
				0.2					0.7018
						1			0.7018
						2			0.6975
						3			0.6936

							1		0.7018
							2		0.7039
							3		0.7045
								0.5	0.4747
								1	0.7018
								1.5	0.8755

References

- [1] Ali B, Ali L, Abdal S, Asjad MI. Significance of Brownian motion and thermophoresis influence on dynamics of Reiner-Rivlin fluid over a disk with non-Fourier heat flux theory and gyrotactic microorganisms: A Numerical approach. *Phys Scr* 2021;96:094001. <https://doi.org/10.1088/1402-4896/AC02F0>.
- [2] Abdal S, Mariam A, Ali B, Younas S, Ali L, Habib D. Implications of bioconvection and activation energy on Reiner–Rivlin nanofluid transportation over a disk in rotation with partial slip. *Chinese Journal of Physics* 2021;73:672–83. <https://doi.org/10.1016/j.cjph.2021.07.022>.
- [3] Alarabi TH, Mahdy A, Abo-zaid OA. Distinctive approach for MHD natural bioconvection flow of Reiner–Rivlin nano-liquid due to an isothermal sphere. *Case Studies in Thermal Engineering* 2024;55:104179. <https://doi.org/10.1016/j.csite.2024.104179>.
- [4] Puspanathan S, Naganthran K, Hashmi MM, Hashim I, Momani S. Numerical investigation of Reiner–Rivlin fluid flow and heat transfer over a shrinking rotating disk. *Chinese Journal of Physics* 2024;88:198–211. <https://doi.org/10.1016/j.cjph.2024.01.021>
- [5] Usman Rashid M, Mustafa M. A study of heat transfer and entropy generation in von Kármán flow of Reiner-Rivlin fluid due to a stretchable disk. *Ain Shams Engineering Journal* 2021;12:875–83. <https://doi.org/10.1016/J.ASEJ.2020.06.017>
- [6] Khan SU, Adnan, Ramesh K, Riaz A, Awais M, Bhatti MM. Insights into the impact of Cattaneo-Christov heat flux on bioconvective flow in magnetized Reiner-Rivlin nanofluids. *Sep Sci Technol* 2024;59:1172–82. <https://doi.org/10.1080/01496395.2024.2366889>
- [7] Sabu AS, Mackolil J, Mahanthesh B, Mathew A. Reiner-Rivlin nanomaterial heat transfer over a rotating disk with distinct heat source and multiple slip effects. *Applied Mathematics and Mechanics (English Edition)* 2021;42:1495–510. <https://doi.org/10.1007/s10483-021-2772-7/metrics>.
- [8] Khan SA, Hayat T, Alsaedi A. Bioconvection entropy optimized flow of Reiner-Rivlin nanofluid with motile microorganisms. *Alexandria Engineering Journal* 2023;79:81–92. <https://doi.org/10.1016/j.aej.2023.07.069>.
- [9] Moatimid GM, Mohamed MAA, Elagamy K. Heat and mass flux through a Reiner–Rivlin nanofluid flow past a spinning stretching disc: Cattaneo–Christov model. *Scientific Reports* 2022 12:1 2022;12:1–24. <https://doi.org/10.1038/s41598-022-18609-7>.
- [10] Khan SA, Hayat T, Alsaedi A. Irreversibility analysis in hydromagnetic Reiner-Rivlin nanofluid with quartic autocatalytic chemical reactions. *International Communications in Heat and Mass Transfer* 2022;130:105797. <https://doi.org/10.1016/j.icheatmasstransfer.2021.105797>.

- [11] Lv YP, Gul H, Ramzan M, Chung JD, Bilal M. Bioconvective Reiner–Rivlin nanofluid flow over a rotating disk with Cattaneo–Christov flow heat flux and entropy generation analysis. *Scientific Reports* 2021;11:1–18. <https://doi.org/10.1038/s41598-021-95448-y>.
- [12] Khan M, Salahuddin T, Alwan B Al. Significance of binary chemical reaction, enthalpy and variable thermophysical properties over a radioactive heated rotated disk. *Chinese Journal of Physics* 2022;77:511–20. <https://doi.org/10.1016/j.cjph.2022.03.015>.
- [13] Ramasekhar G, Ahmad H, Uzun Ozsahin D, Alotaibi MF. Aviation aspects of engine oil conveying copper tiny particles embedded in a rotating disk with a binary chemical reaction. *Case Studies in Thermal Engineering* 2024;63:105180. <https://doi.org/10.1016/j.csite.2024.105180>.
- [14] Shafique Z, Mustafa M, Mushtaq A. Boundary layer flow of Maxwell fluid in rotating frame with binary chemical reaction and activation energy. *Results Phys* 2016;6:627–33. <https://doi.org/10.1016/j.rinp.2016.09.006>.
- [15] Ijaz Khan M, Nasir T, Hayat T, Khan NB, Alsaedi A. Binary chemical reaction with activation energy in rotating flow subject to nonlinear heat flux and heat source/sink. *J Comput Des Eng* 2020;7:279–86. <https://doi.org/10.1093/jcde/qwaa023>.
- [16] Ahmad L, Islam S, Alqahtani AM, Sarfraz M. Swirling motion of temperature-dependent chemical reactions and Arrhenius activation energy in Cross fluid. *International Communications in Heat and Mass Transfer* 2024;159:108082. <https://doi.org/10.1016/j.icheatmasstransfer.2024.108082>.
- [17] Sahoo A, Nandkeolyar R. Radiative heat transport of Cattaneo–Christov double diffusive Casson nanofluid flow between two rotating disks with Hall current and activation energy. *ZAMM - Journal of Applied Mathematics and Mechanics / Zeitschrift Für Angewandte Mathematik Und Mechanik* 2024;104:e202200419. <https://doi.org/10.1002/zamm.202200419>.
- [18] Madhu J, Madhukesh JK, Sarris I, Prasannakumara BC, Ramesh GK, Shah NA, et al. Influence of quadratic thermal radiation and activation energy impacts over oblique stagnation point hybrid nanofluid flow across a cylinder. *Case Studies in Thermal Engineering* 2024;60:104624. <https://doi.org/10.1016/j.csite.2024.104624>.
- [19] Jiann LY, Mohamad AQ, Rawi NA, Chaun Ching DL, Mohd Zin NA, Shafie S. Thermal analysis of melting effect on Carreau fluid flow around a stretchable cylinder with quadratic radiation. *Propulsion and Power Research* 2024;13:132–43. <https://doi.org/10.1016/j.jprr.2024.02.006>.
- [20] Lavanya B, Kumar JG, Babu MJ, Raju CSK, Almutairi B, Shah NA. Entropy generation minimization in the Carreau nanofluid flow over a convectively heated inclined plate with quadratic thermal radiation and chemical reaction: A Stefan blowing application. *Propulsion and Power Research* 2024;13:233–44. <https://doi.org/10.1016/j.jprr.2024.04.004>.

- [21] Rana P, Gupta S, Gupta G. Unsteady nonlinear thermal convection flow of MWCNT-MgO/EG hybrid nanofluid in the stagnation-point region of a rotating sphere with quadratic thermal radiation: RSM for optimization. *International Communications in Heat and Mass Transfer* 2022;134:106025. <https://doi.org/10.1016/j.icheatmasstransfer.2022.106025>.
- [22] Al-Kouz W, Mahanthesh B, Alqarni MS, Thriveni K. A study of quadratic thermal radiation and quadratic convection on viscoelastic material flow with two different heat source modulations. *International Communications in Heat and Mass Transfer* 2021;126:105364. <https://doi.org/10.1016/j.icheatmasstransfer.2021.105364>.
- [23] Islam N, Pasha AA, Jamshed W, Ibrahim RW, Alsulami R. On Powell-Eyring hybridity nanofluidic flow based Carboxy-Methyl-Cellulose (CMC) with solar thermal radiation: A quadratic regression estimation. *International Communications in Heat and Mass Transfer* 2022;138:106413. <https://doi.org/10.1016/j.icheatmasstransfer.2022.106413>.
- [24] Mahanthesh B, Mackolil J, Radhika M, Al-Kouz W, Siddabasappa. Significance of quadratic thermal radiation and quadratic convection on boundary layer two-phase flow of a dusty Nano liquid past a vertical plate. *International Communications in Heat and Mass Transfer* 2021; 120: 105029. <https://doi.org/10.1016/j.icheatmasstransfer.2020.105029>.
- [25] Sarkar A, Mandal G, Pal D. Heat transfer inspection and entropy optimization in water/MoS₂-SiO₂ Casson hybrid nanofluid flow with quadratic radiation ray over an exponentially contracting permeable Riga surface: Duality and stability analysis. *Thermal Advances* 2024;1:100003. <https://doi.org/10.1016/j.thradv.2024.100003>.
- [26] Ali F, Zaib A, Loganathan K, Saeed A, Seangwattana T, Kumam P, et al. Scrutinization of second law analysis and viscous dissipation on Reiner-Rivlin Nanofluid with the effect of bioconvection over a rotating disk. *Heliyon* 2023;9:e13091. <https://doi.org/10.1016/j.heliyon.2023.e13091>